RESEARCH ARTICLE | FEBRUARY 05 2019

Coupled flow and fiber orientation analysis for 3D injection molding simulations of fiber composites FREE

Huan-Chang Tseng ✉; Tung-Huan Su

AIP Conf. Proc. 2065, 030021 (2019)
https://doi.org/10.1063/1.5088279

Coupled Flow and Fiber Orientation Analysis for 3D Injection Molding Simulations of Fiber Composites

Huan-Chang Tseng[a)] and Tung-Huan Su

CoreTech System (Moldex3D) Co., Ltd., ChuPei City, Hsinchu County, 30265, Taiwan.

[a)] Corresponding Author: ivortseng@moldex3d.com

Abstract. In the past, many injection molding simulations based on the Hele-Shaw approximation to predict fiber orientation have been developed. Some researchers have also performed the coupling analysis of flow field and fiber orientation by the Lipscomb constitutive equation of fiber suspension rheology, and demonstrated the close agreement between the coupled and decoupled solutions. At present, the 3D numerical techniques has been widely applied in engineering practices. The primary purpose of this paper is to understand the effect of the coupling and its importance especially in the 3D numerical computation of the injection molded fiber composites.

Keywords: Fiber Composites; Fiber Orientation; Injection Molding Simulation; Flow/Orientation Coupling Analysis; Moldex3D.

Introduction

Fiber reinforced thermoplastic (FRT) composites are lightweight materials widely used in the automotive industry with safety and durability, and can be processed by conventional processing, such as injection molding and compression molding. Primarily, their mechanic properties depend fiber orientation state. During the injection processing, the shell-core orientation structure is important for fiber-reinforced melts. Many simulations have been developed to predict the fiber orientation distribution. Following the famous Folgar-Tucker models [1-2] in the field of fiber orientation, Tseng *et al.* [3] developed a new fiber orientation model, namely, iARD-RPR (improved ARD model and Retarding Principal Rate model) with three physically meaningful parameters. It is later incorporated in the commercial mold-processing simulation software, Moldex3D. Recently, the iARD-RPR model has been demonstrated for various fiber composites with respect to different polymer matrices, higher/lower fiber concentration and carbon/glass fiber, as well as plate and disk with different gate types [4-6]. However, all of those simulations neglected the effect of fiber orientation on filling flow are not accurate enough especially for high-fiber-content reinforced composites.

A flow-induced fiber orientation plays an important role in the flow during a mold filling process, while the flow field is in turn affected by fiber orientation. Early, Lipscomb *et al.* [7-8] developed a constitutive equation of dilute fiber suspensions in which the effect of fiber orientation on flow stress can be modeled:

$$\boldsymbol{\tau} = 2\eta_m \mathbf{D} + 2\eta_m \phi N_p \mathbf{D} : \mathbf{A}_4 \tag{1}$$

where $\boldsymbol{\tau}$ is the extra stress tensor; $\mathbf{D}$ is the rate-of-deformation tensor; η_m is the matrix viscosity; ϕ is the fiber volume fraction; N_p is a dimensionless parameter. The fourth-order orientation tensor $\mathbf{A}_4$ is determined by using a higher order polynomial closure approximation in terms of the second-order orientation tensor $\mathbf{A}$, such as the Eigenvalue-Based Optimal Fitting (EBOF) Closure [9] and the Invariant-Based Optimal Fitting (IBOF) Closure [10]. Note that N_p =0 indicates the decoupling calculation in absence of the fiber orientation effect. A decoupled approach has been availably applied in which the fluid flow problem is first solved, and the resulting velocity field is used to compute the fiber orientation.

Great efforts have been made by many researchers [11-13] for coupling flow stress and fiber orientation calculation of Lipscomb equation performed by the Hele-Shaw approximation. Previously, VerWeyst and Tucker [12] have demonstrated in injection molding simulations of the center-gated disk that the fiber orientation tensor components are independent of the parameter N_p, while the velocity profile are almost not varied. For this point, we therefore aim that the coupled approach is validated in 3D-numerical computation of the Moldex3D injection molding simulation. The melt front, velocity profile and fiber orientation distribution are presented, as well

Proceedings of PPS-34
AIP Conf. Proc. 2065, 030021-1–030021-5; https://doi.org/10.1063/1.5088279
Published by AIP Publishing. 978-0-7354-1793-9/$30.00

Polymer Fluid Mechanics

For injection-molded fiber composites, the actual flow of the fibers dispersed in the polymer melt is transient, non-Newtonian and non-isothermal, as the complex mixture squeezes into the mold cavity. The process is highly nonlinear, as the material properties are dependent upon the rheological and thermal conditions. In addition, the effect of fiber orientation upon the flow behavior is critical. The polymeric melts with fiber suspensions are generally assumed as Generalized Newtonian Fluids (GNF) [14]. The governing equations of the fluid mechanics which describe the transient and non-isothermal flow motion are as follows:

$$\frac{\partial \rho}{\partial t} + \nabla \cdot \rho \mathbf{u} = 0 \tag{2}$$

$$\frac{\partial}{\partial t}(\rho \mathbf{u}) + \nabla \cdot (\rho \mathbf{u}\mathbf{u} - \boldsymbol{\sigma}) = \rho \mathbf{g} \tag{3}$$

$$\boldsymbol{\sigma} = -p\mathbf{I} + \boldsymbol{\tau} \tag{4}$$

$$\rho C_P \left(\frac{\partial T}{\partial t} + \mathbf{u} \cdot \nabla T \right) = \nabla \cdot (k \nabla T) + \eta \dot{\gamma}^2 \tag{5}$$

where ρ is density; $\mathbf{u}$ is velocity vector; t is time; $\boldsymbol{\sigma}$ is total stress tensor; $\boldsymbol{\tau}$ is the extra stress tensor; $\mathbf{g}$ is acceleration vector of gravity; p is pressure; η is the isotropic viscosity; C_p is specific heat; T is temperature; k is thermal conductivity; $\dot{\gamma}$ is shear rate. Tait's PVT model [15] is to express a thermodynamic state relationship, namely, the volume of the material as a function of the temperature and pressure. The Cross-William-Landel-Ferry (Cross-WLF) model [14] can describe complex viscosity behaviors, including the viscosity varying with shear rate for the Cross model and the zero-shear-rate viscosity depending on temperature and pressure for the WLF model.

In this work, flow field is computed with reference to fiber orientation by the Lipscomb equation of **Eq. (1)** and then those flow fields are used to determine the fiber orientation state; this is the coupling flow-fiber computation. Note that the Lipscomb parameter $N_p = 0$ is given in, so that the Lipscomb stress becomes the GNF stress, namely the decoupling calculation in absence of the fiber orientation effect,

$$\boldsymbol{\tau} = 2\eta \mathbf{D} \tag{6}$$

Fiber Orientation Kinetics

A single fiber is regarded axisymmetric and rigid. The bond's unit vector $\mathbf{p}$ along its axis direction can describe fiber orientation. Advani and Tucker [16] defined the second order orientation tensor as:

$$\mathbf{A} = \oint \psi(\mathbf{p}) \mathbf{p}\mathbf{p} \, d\mathbf{p} \tag{7}$$

where $\psi(\mathbf{p})$ is the probability density distribution function over orientation space.

Tseng *et al.* [3] developed a new fiber orientation model to couple with Jeffery's hydrodynamic (HD) model, namely, the iARD-RPR model (known as Improved Anisotropic Rotary Diffusion model combined with Retarding Principal Rate model),

$$\dot{\mathbf{A}} = \dot{\mathbf{A}}_{\mathrm{HD}} + \dot{\mathbf{A}}_{\mathrm{iARD}}(C_I, C_M) + \dot{\mathbf{A}}_{\mathrm{RPR}}(\alpha) \tag{8}$$

where $\dot{\mathbf{A}}$ represents the material derivative of $\mathbf{A}$. C_I and C_M describe the fiber-fiber interaction and fiber-matrix interaction, respectively; α can slow down a response of fiber orientation. Details of the RPR and iARD models are described in reference. According to these criteria, we can fine-tune three parameters to obtain an accurate orientation prediction, namely, determining an optimal parameter set. The shell-orientation layer depends on the iARD parameters (C_I and C_M), while the core region and skin layer are controlled by the RPR parameter (α). For the range of these three parameters, the best practices are: $0 < C_I < 0.1$; $0 < C_M < 1$; $0 < \alpha < 1$. When C_M and α all set to 0, iARD-RPR model goes back to Folgar-Tucker model [3].

Results and Discussion

In this work, the Lipscomb equation of coupling flow-fiber [see **Eq. (1**] has been implemented in Moldex3D software. One case study that is a center-gated disk mold filling is shown in **Figure 1**. The disk is 90 mm in radius with a thickness of $2h$ = 3 mm. The 3-D model was first developed by one of the CAD (Computer Aided Design) programs and then meshed by creating hexagonal elements with 20 layers. The 40wt% long glass-fiber immersed in a polypropylene matrix (denoted as 40wt% LGF/PP) is used. A volume flow rate is 118.32cm^3/sec with a filling time of 0.65 sec. All of details are available elsewhere [17-18].

First, we applied Moldex3D to simulate the center-gated disk flow for the 40wt% LGF/PP fluid, and then examined the Lipscomb equation at different N_p values, including N_p = 0, 10, and 20, as shown in **Figure 2**. When giving N_p =0, the Lipscomb stress becomes the GNF stress independent upon fiber orientation, namely the decoupling calculation in absence of the fiber orientation effect. That is, the flow field is computed without reference to fiber orientation and then those flow fields are used to determine the fiber orientation state. We found the perfect circle-shape melt front of the isotropic flows for the decupling result (set N_p =0) and the coupling of using N_p = 10. However, there is the divergent calculation finished as giving a large value, N_p = 20.

Moreover, there is one measurement point located at the middle point along the radial direction, as shown in **Figure 1**. We found the same perfect circle-shape melt front of the isotropic flows for the decupling result and the coupling of using N_p = 10. However, there is the divergent calculation finished as giving a large value, N_p = 20. At this point, **Figure 3 and Figure 4** show the average velocity profile and the flow-direction fiber orientation A11 distribution through the normalized thickness performed by different values of the Lipscomb parameter N_p, respectively. It is clear that the velocity profile almost does not change with respect to N_p. In fiber orientation distribution, the shell layer for the coupling is somewhat lower than for the decoupling and the core region does not varied. However, these predicted orientation results are not accurate enough for high fiber concentrations of long fiber composites. In addition, **Figure 5** shows changes in the sprue pressure with filling time. The pressure for the coupling is slight high than for decoupling. This finding is in consistence with the previous study of VerWeyst and Tucker. Overall, the coupling flow-fiber result of using 3D numerical calculation is similar to using the Hele-Shaw approximation.

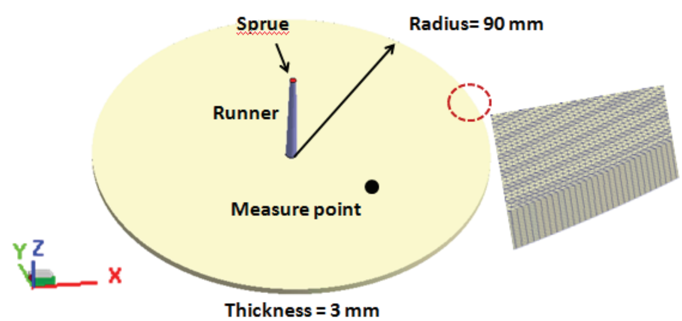

Figure 1. Illustration of injection molding simulation of the center-gated disk.

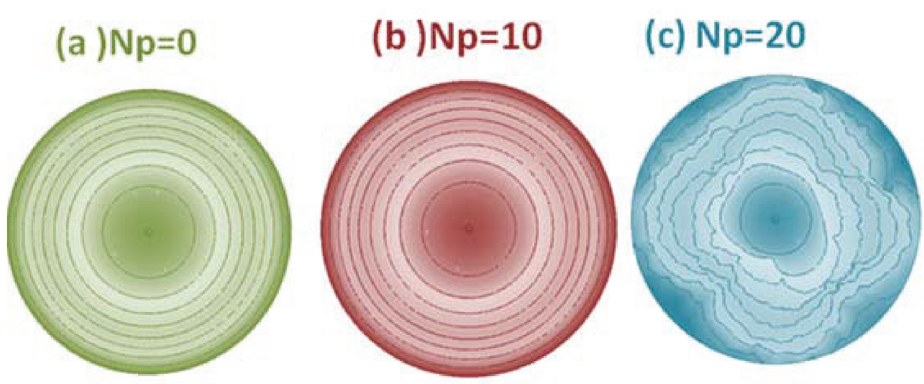

Figure 2. Melt fronts of the center-gated disk flow for different N_p values.

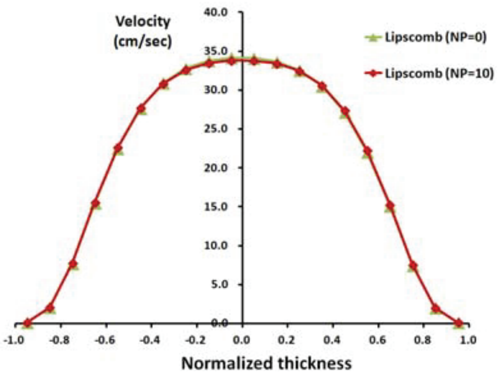

Figure 3. The average velocity profile at the middle point along the radial direction for different N_p values.

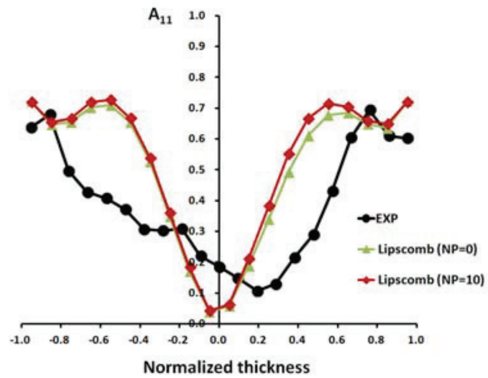

Figure 4. The flow-directional orientation component A11 distribution for different N_p values.

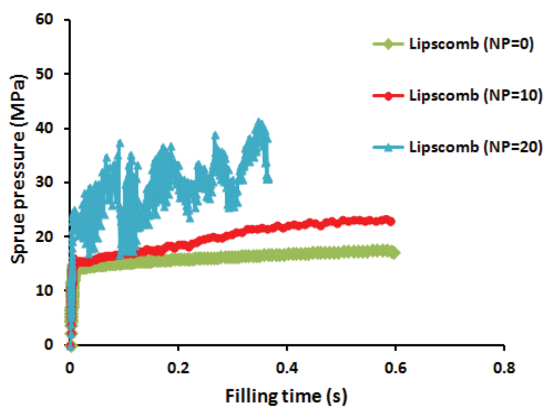

Figure 5. Changes in sprue pressure with respect to filling time for different N_p values.

Conclusion

In this work, we verified that the fiber orientation predictions for the Lipscomb equation of coupling flow-fiber performed in the 3D numerical computation of injection molding simulation are unsatisfactory. As a comparison of the decoupling and the coupling, the velocity profile and the orientation distribution do almost not vary with increasing the parameter N_p. However, it is critical to easily get a divergent result when giving a large the parameter N_p. In future work, we are going to primarily improve the Lipscomb equation to simulate the fiber-induced anisotropic flow of fiber-reinforced melts during injection molding and compression molding.

References

[1] Folgar F, Tucker III CL. Orientation behavior of fibers in concentrated suspensions. J Reinf Plast Compos 1984; 3(2) 98-119.

[2] Advani SG, Tucker III CL. A numerical simulation of short fiber orientation in compression molding. Polym Compos 1990; 11 164-173.

[3] Tseng H-C, Chang R-Y, Hsu C-H. An objective tensor to predict anisotropic fiber orientation in concentrated suspensions. J Rheol 2016; 60(2) 215-224.

[4] Foss PH, Tseng H-C, Snawerdt J, Chang Y-J, Yang W-H, Hsu C-H. Prediction of fiber orientation distribution in injection molded parts using moldex3d simulation. Polym Compos 2014; 35(4) 671-680.

[5] Tseng H-C, Chang R-Y, Hsu C-H. Numerical prediction of fiber orientation and mechanical performance for short/long glass and carbon fiber-reinforced composites. Compos Sci and Technol 2017; 144 51-56.

[6] Tseng H-C, Chang R-Y, Hsu C-H. Improved fiber orientation predictions for injection molded fiber composites. Composites Part A: Applied Science and Manufacturing 2017; 99 65-75.

[7] Lipscomb II GG, Denn MM, Hur DU, Boger DV. The flow of fiber suspensions in complex geometries. J Non-Newtonian Fluid Mech 1988; 26 297-325.

[8] Wang J, O'Gara JF, Tucker III CL. An objective model for slow orientation kinetics in concentrated fiber suspensions: Theory and rheological evidence. J Rheol 2008; 52(5) 1179-1200.

[9] VerWeyst BE. Numerical predictions of flow-induced fiber orientation in three-dimensional geometries. Urbana-Champaign: Ph.D. Thesis, University of Illinois; 1998.

[10] Chung DH, Kwon TH. Invariant-based optimal fitting closure approximation for the numerical prediction of flow-induced fiber orientation. J Rheol 2002; 46(1) 169-194.

[11] Chung ST, Kwon TH. Coupled analysis of injection molding filling and fiber orientation including in-plane velocity gradient effect. Polym Compos 1996; 17 859-872.

[12] VerWeyst BE, Tucker III CL. Fiber suspensions in complex geometries: Flow/orientation coupling. Can J Chem Eng 2002; 80(6) 1093-1106.

[13] Mazahir SM, Vélez-García GM, Wapperom P, Baird DG. Evolution of fiber orientation in radial direction in a center-gated disk: Experiments and simulation. Compos Pt A-Appl Sci Manuf 2013; 51 108-117.

[14] Bird RB, Armstrong RC, Hassager O. Fluid mechanics. 2nd ed. New York: Wiley-Interscience, 1987.

[15] Chang R-Y, Chiou S-Y. A unified k-bkz model for residual stress analysis of injection molded three-dimensional thin shapes. Polym Eng Sci 1995; 35(22) 1733-1747.

[16] Advani SG, Tucker III CL. The use of tensors to describe and predict fiber orientation in short fiber composites. J Rheol 1987; 31(8) 751-784.

[17] Nguyen N, Jin X, Wang J, Phelps JH, Tucker III CL, Kunc V, Bapanapalli SK, Smith MT. Implementation of new process models for tailored polymer composite structures into processing software packages. the US Department of Energy, Pacific Northwest National Laboratory, PNNL Report under Contract DE-AC05-76RL01830 2010; PNNL-19185.

[18] Tseng H-C, Chang R-Y, Hsu C-H. An integration of microstructure predictions and structural analysis in long-fiber-reinforced composite with experimental validation. Int Polym Process 2017; 32 455-466.